arXiv:2209.02858v2 [cond-mat.mes-hall] 11 Apr 2023

A Physical Model for Drain Noise in High Electron Mobility Transistors: Theory and Experiment

Bekari Gabritchidze, Kieran A. Cleary, Anthony C. Readhead, Austin J. Minnich

***Abstract*—We report the on-wafer characterization of S-parameters and microwave noise temperature (T_{50}) of discrete metamorphic InGaAs high electron mobility transistors (mHEMTs) at 40 K and 300 K over a range of drain-source voltages (V_{DS}). From these data, we extract a small-signal model and the drain noise temperature (T_d) at each bias and temperature which accounts for the variation of small-signal model parameters, noise impedance match, and noise generator temperatures under the various conditions. We find that T_d follows a non-linear trend with V_{DS} at both temperatures. These trends are interpreted by attributing drain noise to a thermal component associated with the channel resistance and a component due to real-space transfer (RST) of electrons from the channel to the barrier. Using this noise model, we find that RST contributes $\lesssim 5\%$ to the drain noise at cryogenic temperatures when biased for minimum noise temperature. At 300 K, the contribution increases to over $\sim 60\%$ of the total drain noise. This finding suggests that improving the confinement of electrons in the quantum well could enable room-temperature receivers with up to $\sim 30\%$ lower noise temperatures by decreasing the contribution of RST to drain noise.**

***Index Terms*—High electron mobility transistors, cryogenic electronics, microwave noise, low-noise amplifiers, drain temperature, real-space transfer**

I. INTRODUCTION

HIGH electron mobility transistors are widely employed in microwave amplifiers due to their low noise characteristics [1], [2], [3]. While significant improvements have been made in their noise and frequency performance in past decades [4], [5], [6], [7], a physics-based understanding of the origin of microwave noise is lacking. Presently, noise in HEMTs is interpreted with the Pospieszalski model [8] in which noise is described using two uncorrelated noise generators associated with the gate and drain resistances R_{gs}, R_{ds} with equivalent temperatures T_g, T_d, respectively. T_g is modelled as the physical temperature (T_{ph}) of the gate, while T_d is used as a fitting parameter and is on the order of 1000 K. Despite the utility of this model, it is unable to provide insight into the physical origin of T_d.

Recently, a drain noise model based on suppressed shot noise was proposed [9]. This model required the output noise power to be temperature-independent, but this prediction has been found to be inconsistent with experiments [10], [11]. A new theory attributes drain noise to microwave partition noise arising from real-space transfer (RST) [12], a process that has been intensively investigated in early studies of transport and noise in quantum wells [13], [14]. In this mechanism, electrons are heated by the electric field under the gate to physical temperatures exceeding 1000 K, a temperature sufficiently high that some electrons may thermionically emit out of the channel into the barrier. Because the barrier mobility is substantially less than that of the channel, two dissimilar conduction pathways exist from source to drain, creating partition noise. The theory makes several predictions, among them the dependence of T_d on physical temperature. A recent study using on-wafer characterization of discrete HEMTs observed the predicted temperature dependence of T_d [11], and other works have reported similar trends [10], [15], [16]. Additional dependencies of T_d have been observed experimentally, such as dependence on I_{DS} [10], [17], [18], [19] and V_{DS} [10], [19]. Despite these various experimental observations, the physical origin of drain noise in HEMTs remains a topic of debate.

In this paper, we performed on-wafer S-parameter and microwave noise measurements (T_{50}) of discrete metamorphic InGaAs mHEMTs at 40 K and 300 K and various V_{DS} using a cryogenic probe station [11], [20]. At each temperature and bias we extracted a small-signal model (SSM) and noise parameters from the S-parameter and T_{50} measurements, allowing for the determination of drain noise temperature (T_d) while accounting for changes in small-signal parameters and optimal noise impedance at each condition. We find that T_d must depend on V_{DS} and T_{ph} to explain the measured noise temperature trends. These dependencies can be explained by considering drain noise to originate from a thermal component associated with the electron temperature in the channel, and another component arising from RST that depends exponentially on V_{DS} and T_{ph}. This analysis predicts that the non-thermal component of the noise may contribute over half of the total drain noise at 300 K. If this contribution were suppressed, the minimum noise temperatures (T_{min}) would be 30% lower at the low-noise bias. Additional investigation of the role RST may play in drain noise is therefore a topic of interest.

This paper is organized as follows. A brief description of the experimental set up and the modeling is presented in Section II. The S-parameter and microwave noise characterization and the extracted drain temperatures are presented in Section III. A model for drain temperature is presented in Section IV, followed by a discussion of its implications in

---

This work was supported by the National Science Foundation under Grant No. 1911220.(*Corresponding author: A. Minnich*)

B. Gabritchidze is with the Division of Physics, Mathematics and Astronomy, California Institute of Technology, Pasadena, CA, 91125, and also with the Department of Physics, University of Crete, GR-70013 Heraklion, Greece (bekari@caltech.edu)

K. A. Cleary and A. C. Readhead are with the Division of Physics, Mathematics and Astronomy, California Institute of Technology, Pasadena, CA, 91125.(kcleary@astro.caltech.edu, acr@astro.caltech.edu)

A. J. Minnich is with Division of Engineering and Applied Science, California Institute of Technology, Pasadena, CA, 91125(aminnich@caltech.edu)

Section V. Finally, we provide a summary of the paper in Section VI.

II. ON WAFER CRYOGENIC CHARACTERIZATION AND MODELING

The S-parameters and the microwave noise temperature of metamorphic InGaAs mHEMTs (OMMIC, D007IH, 4F50, gate length $L_g = 70$ nm) were measured using a cryogenic probe station (CPS) [20]. Details of the measurement procedure and the experimental set-up were described earlier [11]. In brief, the S-parameter measurements were carried out in the frequency range 1 – 18 GHz using a vector network analyzer (VNA, Rhode & Schwartz ZVA50). The system was calibrated by transferring the measurement plane from the VNA to the tips of the wafer probes (GGB industries, 40A-GSG-100-DP) by through-reflect-match (TRM) calibration on a CS-5 calibration substrate (GGB Industries).

The microwave noise was measured using the Y-factor method with a cold attenuator [11], [21] at a generator impedance of 50 Ω. The CPS was configured for noise measurements from 2$-$18 GHz, however, the measurement bandwidth was chosen from 5$-$15 GHz to minimize RF probe$-$pad contact time and avoid RF pad damage due to chuck vibrations. A 10 dB cryogenic and a room temperature attenuator (Quantum Microwave) were inserted between the noise source (Keysight, N4002A) and the device under test (DUT). The room-temperature attenuator was connected directly to the noise source (NS) to reduce the change in output reflections from the 'on' to 'off' state of the NS, while the cryogenic attenuator was connected to the RF input probe contacting the input of the DUT and served as a cold load. After the DUT, a cryogenic amplifier (Cosmic Microwave, CIT1-18) was used after the output probe within the probe station, and a combination of mixer, oscillator, filters, amplifiers and a power sensor were used outside the probe station to further process and measure the incident noise power. A detailed schematic was presented in [11].

An analysis indicated that the uncertainty in noise temperature arose primarily from uncertainty in the input loss. These losses consist of stainless steel coaxial cable, cryogenic 10 dB attenuator, cryogenic bias tee, and the input RF probe. These losses were characterized in a separate cryogenic dewar at each temperature for which noise measurements were performed. The insertion loss of the input RF probe was measured at room temperature by measuring the return loss with the probe tips open, but could not be measured at cryogenic temperatures. Therefore, an uncertainty of 0.1 dB on the input loss was assumed for the RF probe to account for any changes in its insertion loss as T_{ph} is decreased from 300 K to 40 K. Its temperature was assumed to be that of the cryogenic bias tee connected to the RF probe. While certainly of importance for absolute noise temperature values, these uncertainties only uniformly shift the measured T_{50} and thus do not affect the trends of T_{50} with V_{DS} at any T_{ph}. Based on an uncertainty of 0.1 dB in the input loss, an absolute uncertainty of $\sim 20\%$ at $T_{ph} = 40$ K and $\sim 15\%$ at $T_{ph} = 300$ K in T_{50} was determined. The repeatability of the T_{50} measurements was $\lesssim 0.5$ K at $T_{ph} = 40$ K and ~ 1 K at $T_{ph} = 300$ K.

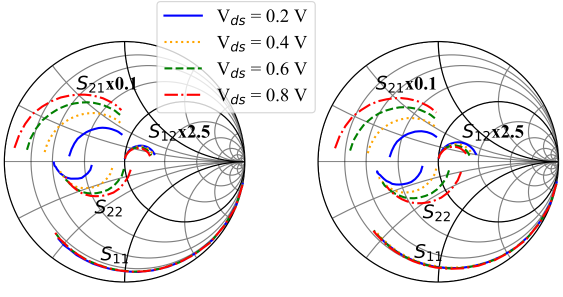

(a) (b)

Fig. 1: Measured S-parameters versus frequency over 1 – 18 GHz at various V_{DS} and physical temperatures of 40 K (a) and 300 K (b).

From the S-parameter and T_{50} measurements, a small-signal model (SSM) was developed. First, the parasitics were extracted through cold-FET measurements following [22], [23], [24], [25], [26]. Once the parasitics were determined and de-embedded, the intrinsic parameters were evaluated by direct extraction and optimization of the intrinsic parameters. Simulated annealing and quasi-Newton optimization, available in Advanced Design System (ADS, Keysight), were used to minimize a least-square error function following [11], [27]. After the optimization, the intrinsic parameters were further fine tuned to improve the agreement between the measured and simulated $S-$parameters. Temperature independence of the extracted parasitic capacitances and inductances was assumed based on [10], [25], and the 300 K values were used at all T_{ph}. The parasitic resistances (R_g, R_s, R_d) have been reported to vary ~ 50 % as T_{ph} is decreased from 300 K to 40 K [25]; however, these resistances are difficult to measure at cryogenic temperatures. We estimated the effect of decreasing parasitic resistances by 50% in the 40 K SSM on SSM parameters and T_d and found that this change altered g_m and R_{ds} by $\sim 5\%$ and T_d by $\sim 2\%$. Therefore, we neglected the temperature dependence of the parasitic resistances. Additionally, the parasitics are bias-independent [25], so at a given T_{ph} the observed V_{DS} dependent trends are not affected by the assumption of constant parasitic resistance. However, the absolute values of minimum noise temperature (T_{min}) with V_{DS} at $T_{ph} = 40$ K are overestimated by $\sim 10\%$ at 6 GHz when the parasitic resistance at 300 K is used for all temperatures.

Under these assumptions, a noise model was obtained by fitting the measured and modeled T_{50} using the drain temperature, T_d, as a fitting parameter. This procedure allowed for the variation of T_d with parameters such as bias and temperature to be isolated from changes due to small-signal parameters and optimal source impedance.

III. EXPERIMENTAL RESULTS

Fig. 1 shows the measured S-parameters at various V_{DS} ranging from 0.2 – 0.8 V and physical temperatures of 40 K and 300 K. At a given T_{ph}, S_{21} and S_{22} exhibit the largest variation with V_{DS}, while S_{12} and S_{11} show smaller but observable dependence.

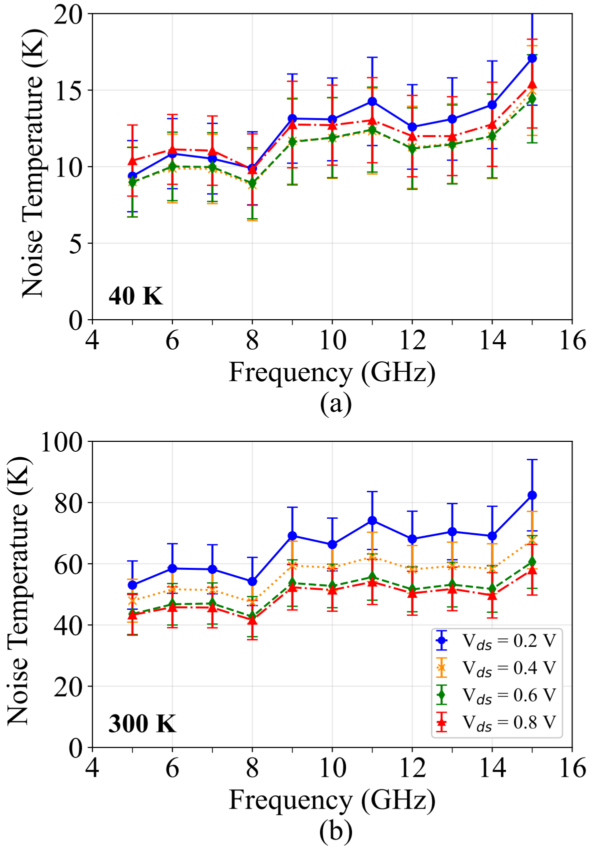

Fig. 2: Measured T_{50} versus frequency at various V_{DS} and physical temperature of 40 K (a) and 300 K (b). The V_{GS} remained constant at all V_{DS} with $V_{GS} = -136$ mV and $V_{GS} = -226$ mV at 40 K and 300 K, respectively.

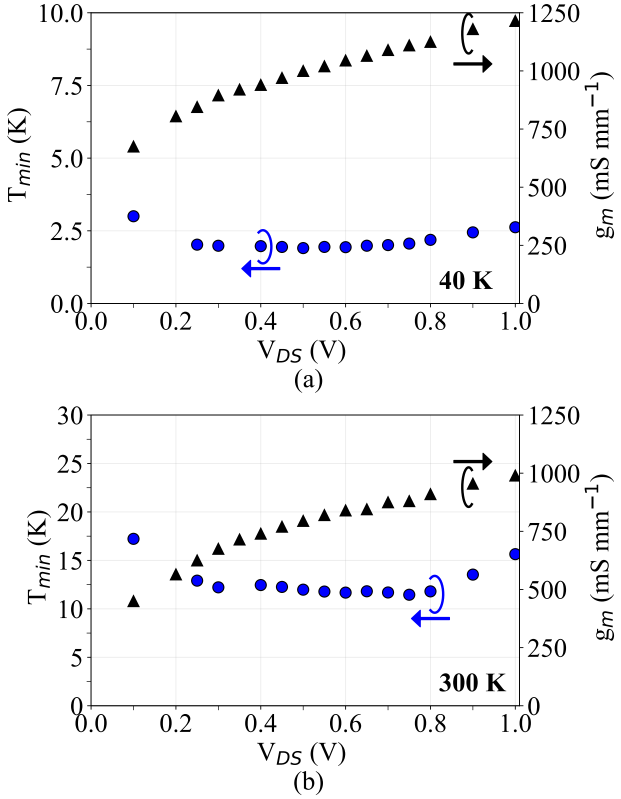

Fig. 3: T_{min} obtained from the noise model created from S-parameter and T_{50} measurements (left y-axis, blue circles) at 6 GHz and measured transconductance g_m (right y-axis, black triangles) at T_{ph} of 40 K (a) and 300 K (b).

In Fig. 2, T_{50} versus frequency is shown for various V_{DS} and the two physical temperatures. In both the S-parameter and noise measurements, the gate voltage (V_{GS}) was kept constant, $V_{GS} = -136$ mV at $T_{ph} = 40$ K, and $V_{GS} = -226$ mV at $T_{ph} = 300$ K, for all V_{DS}. These V_{GS} were selected so that $I_{DS} = 20$ mA at $V_{DS} = 0.8$ V and a given T_{ph}. The V_{DS} was varied from 0.1 V to 1.0 V; V_{DS} was restricted to ≤ 1.0 V so that gate leakage currents (I_G) were $I_G \lesssim 20$ μA/mm at $T_{ph} = 300$ K and the contribution of shot noise was negligible [28]. The lowest T_{ph} was limited to 40 K as self-heating becomes non-negligible for $T_{ph} < 40$ K [29] and T_g is no longer equal to T_{ph}.

Figs. 3a and 3b show modeled T_{min} and the transconductance (g_m) versus V_{DS} at 6 GHz, for physical temperatures of 40 K and 300 K. Similar trends are observed at both temperatures, with the minimum in T_{min} shifting from V_{DS} ~ 0.75 V at 300 K to $V_{DS} \sim 0.5$ V at 40 K. This observation is explained by higher g_m at $T_{ph} = 40$ K than at 300 K for a given V_{DS} and therefore reduced contribution of drain noise to T_{min}. The transconductance g_m increases with increasing V_{DS} but plateaus at $V_{DS} \gtrsim 1.0$ V and both T_{ph}.

Qualitative findings can be obtained from the trend of g_m and T_{min} versus V_{DS}. In particular, at $T_{ph} = 40$ K and as V_{DS} increases above the low noise bias point $V_{DS} = 0.6$ V, both g_m and T_{min} increase. Assuming that self-heating effects can be neglected, the increase in T_{min} despite the increased gain must arise from T_d, indicating that T_d exhibits a dependence on V_{DS}. At bias below the low noise bias, the increase in noise with decreasing V_{DS} is due to reduced gain. A similar variation of g_m, T_{min} and T_d with V_{DS} is observed at 300 K (Figs. 3b and 4b) This dependence cannot be attributed to non-ideal effects like impact ionization, as at all V_{DS} and V_{GS} values the gate–source current, I_{GS}, remained at values between -5 μA/mm and -20 μA/mm. However, impact ionization is often accompanied by a marked increase in gate current (see [3, Fig. 1] and [26, Fig. 6.7]) and occurs in different bias regime than employed here ($V_{GS} > 0$ V, $V_{DS} > 1.0$ V) [26]. Additionally, S_{22} remained capacitive for all V_{DS} [30] while no hump was observed in output conductance [31]. Therefore impact ionization is unlikely to be the origin of the variation of T_d with V_{DS}.

To gain insight into the variation of drain noise with the V_{DS} and T_{ph}, we extract T_d at each bias and temperature using the measured T_{50} and S-parameters. This procedure accounts for changes in small-signal parameters and noise match using the noise model, allowing the variation from only the drain noise to be identified. The extracted T_d versus V_{DS} at 40 K and 300 K is shown in Figs. 4a and 4b. Additional T_d measurements for a similar device from the same wafer reticle are also shown at selected V_{DS}. The extracted T_d follows a linear trend at low

$V_{DS} \lesssim 0.6$ V and rises non-linearly at higher voltages. The error bars for the extracted T_d were determined by calculating T_d for the minimum and maximum values of T_{50} within the error bars and were found to range from ±150 K to ±400 K, depending on physical temperature and the uncertainty in T_{50}.

IV. PHYSICAL MODEL FOR DRAIN NOISE

The extracted drain temperatures exhibit a nonlinear trend as a function of V_{DS} (Fig. 4) at both cryogenic and room temperatures. In our prior work [11] and other works [10], [15], T_d is also observed to depend non-linearly on physical temperature.

We now aim to interpret these trends through a theory of drain noise. A proposed mechanism for drain noise based on a suppressed shot noise theory was suggested in [9] in which T_d was expressed in terms of a temperature-independent suppression factor (Fano factor), g_{ds} and I_{DS}. According to this theory, if I_{DS} is kept constant with physical temperature then the output noise power $T_d g_{ds}$ is predicted to be temperature-independent. This prediction is inconsistent with the measured temperature dependence of the output noise power which changes from ~ 60 pA(Hz mm)$^{-1/2}$ to ~ 90 pA(Hz mm)$^{-1/2}$ as T_{ph} is varied from 40 K to 300 K. This magnitude of variation significantly exceeds the estimated uncertainty in the measured output noise power of $\sim 10\%$, and we therefore conclude that the output noise power must exhibit a dependence on physical temperature. This conclusion is consistent with the findings of [11], [10], [15].

The RST theory for drain noise proposed in [12] predicts T_d to exhibit a temperature dependence. However, the dependence is predicted to be exponential, and the measured trends vary less rapidly than predicted from RST alone. We therefore introduce a model of drain noise based on earlier studies of microwave noise in quantum wells [14] in which the noise arises from two components: the thermal noise associated with the channel resistance and RST. T_d can then be expressed as:

$$T_d = T_e + T_{RST} \tag{1}$$

where the RST noise temperature is given as:

$$T_{RST} = T_{RST}^{o} \exp\left[-(\Delta E_c - q(V_{GS} - V_{th}))/k_B T_e\right] \tag{2}$$

Here, q is the electric charge, k_B the Boltzmann constant, V_{GS} the gate-source voltage, V_{th} the threshold voltage, and ΔE_c the channel-barrier conduction band discontinuity. The temperature dependence of ΔE_c was omitted and was set to ~ 0.685 eV at all T_{ph} [32]. The value of ΔE_c is taken from [32] for a composite channel with In composition of 0.7 and a lattice-matched barrier present in OMMIC devices [33]. From [12, eq. (4)],

$$T_{RST}^{0} = q^2 v_{d1}^2 n_{s1} \tau \gamma W / k_B g_{ds} L_g, \tag{3}$$

where $v_{d1} \sim 4 \times 10^7$ cm s^{-1} is the saturation velocity in the channel [34], $\tau \sim 1$ ps is the characteristic time of electrons to transfer from channel to barrier [12], n_{s1} is the channel electron sheet density (typically $\sim 2 \times 10^{12}$ cm^{-2} [14]), W is the gate width, g_{ds} the drain–source conductance extracted from the small-signal model, $L_g \sim 70$ nm is the gate length, and γ is the probability of hot electrons to emit from channel to barrier. For simplicity, it is assumed that all electrons with energy exceeding ΔE_c transfer to the barrier so that $\gamma = 1$, and that T_{RST}^0 is independent of temperature. The specific values of these parameters do not affect the trends of T_d versus V_{DS} and T_{ph} and so are of secondary importance. In the model, the difference $V_{GS} - V_{th}$ was fixed at $V_{GS} - V_{th} \sim 43$ mV so that at constant $V_{DS} = 0.6$ V and all T_{ph} the $I_{DS} = 10$ mA.

Using (1), we solved for T_{el} and thereby obtained T_{el} and T_{RST}, corresponding to the thermal and RST components of T_d, respectively, at each extracted T_d of Fig. 4. The result is shown in Fig. 4. The obtained T_{el} increases with V_{DS}; however, the rate of increase is reduced and plateaus at $V_{DS} \gtrsim 1.0$ V. We observe that T_{el} and T_d differ by less than 10% for $V_{DS} \lesssim 0.6$ V and $T_{ph} = 40$ K, indicating that RST makes a minor contribution at these V_{DS}. At higher V_{DS} a marked deviation between T_d and T_{el} is observed, indicating the onset of the RST component. At 300 K, T_{el} is higher due to the higher T_{ph}, and as a result, RST starts to contribute to the total drain temperature even at $V_{DS} \sim 0.2$ V.

Fig. 5 shows the temperature-dependence of T_d at various T_{ph} from 40 K to 300 K at $V_{DS} = 0.6$ V and $I_{DS} = 10$ mA first reported in [11]. Using the model for drain noise, we are now able to separate the individual contributions of thermal and RST to T_d. A nearly linear dependence of T_{el} on T_{ph} is observed, as expected, but the RST temperature, T_{RST}, follows a nonlinear trend with T_{ph}, varying from ~ 40 K to ~ 1000 K over the same physical temperature range. The total contribution of RST to T_d varies depending on V_{DS} as in Fig. 4; however, the RST contribution to drain noise increases monotonically and non-linearly as the physical temperature increases. The different values of T_d at $V_{DS} = 0.6$ V of Fig. 4 and Fig. 5 is attributed to different I_{DS}, with higher T_d corresponding to higher I_{DS} [11].

V. DISCUSSION

We now consider our model for drain noise in the context of prior studies of microwave noise in HEMTs and quantum wells. Microwave noise in quantum wells at InAlAs/InGaAs heterojunctions of composite and homogeneous InGaAs and AlGaAs channels has been extensively studied as described in [14, Fig. 17.1]). These devices can be regarded as ungated HEMTs. The measured noise was observed to exhibit a strong dependence on electric field above a certain threshold value which depended on the value of the conduction band offset between the channel and barrier ([14, Fig. 16.12] and [14, Fig. 17.1]), and these trends were attributed to the contribution of thermal noise and RST. The characteristics of the drain noise reported here and their interpretation are therefore consistent with these prior studies of microwave noise in diverse types of III-V quantum wells.

Supposing that drain noise does originate from the contributions of thermal and RST noise, we use our noise model to estimate the magnitude of improvement in T_{min} if the RST contribution were suppressed by improved confinement of electrons in the quantum well. In Fig. 6a, we plot the

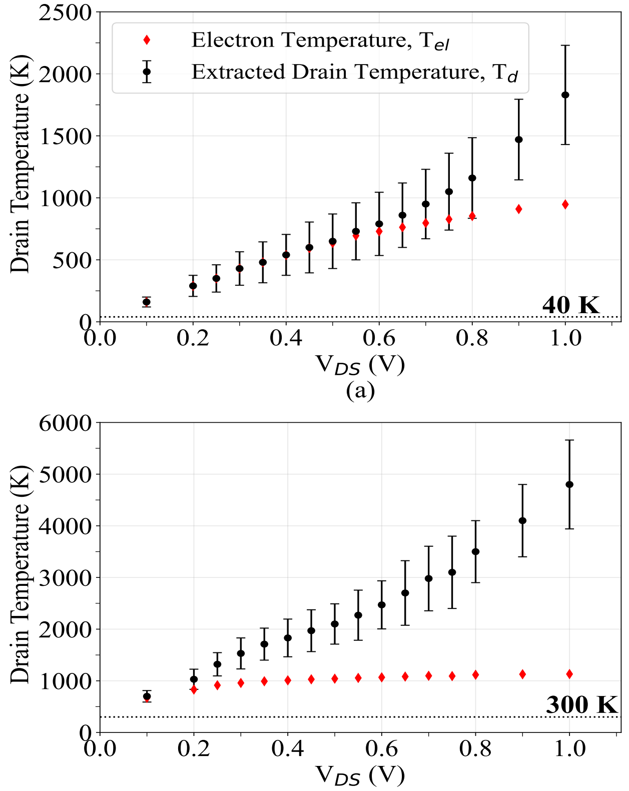

(a)

(b)

Fig. 4: Extracted T_d (black circles) and electron temperature T_{el} (red diamonds) versus V_{DS} based on (1) at 40 K (a) and 300 K (b). The physical temperature, T_{ph} is shown as a comparison in both (a) and (b) as dotted line parallel to V_{DS} axis.

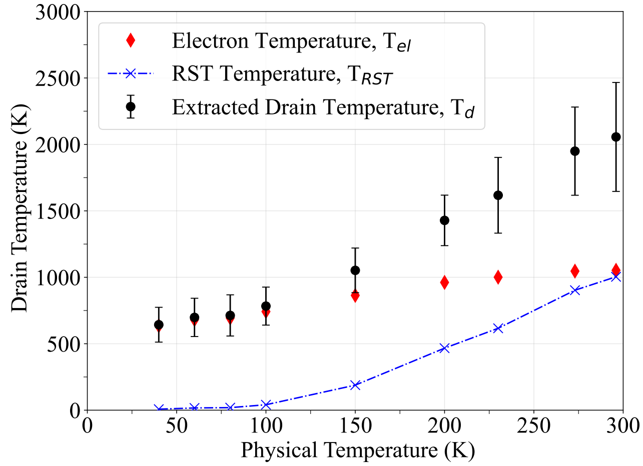

Fig. 5: Extracted drain temperature T_d (black cirlces) versus physical temperature T_{ph} at constant $V_{DS} = 0.6$ V and $I_{DS} = 10$ mA [11]. The electron physical temperature T_{el} (red dashed line and diamond marker) derived by solving (1) and the real space transfer part T_{RST} of (1) (blue dashed dot line cross marker).

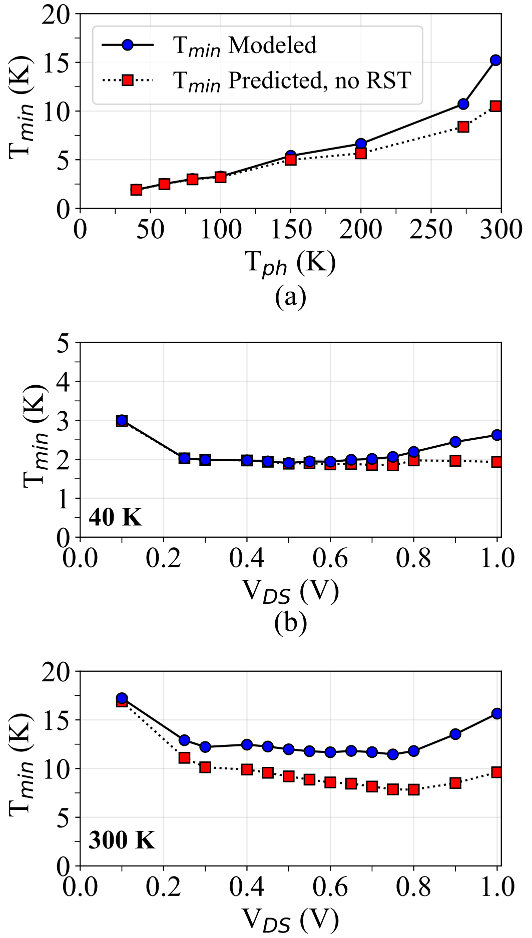

(a)

(b)

(c)

Fig. 6: Modeled T_{min} [11] and predicted T_{min} versus physical temperature at constant $V_{DS} = 0.6$ V and $I_{DS} = 10$ mA (a), and versus V_{DS} at 40 K (b) and 300 K (c) at constant $V_{GS} = -136$ mV and $V_{GS} = -226$ mV, respectively. The predicted T_{min} is modeled by replacing the extracted T_d with T_{el} (i.e. $T_{RST} = 0$) in the noise model. All the above data are at the frequency of 6 GHz. The V_{GS} in (b) and (c) were selected so that at both physical temperatures, $V_{DS} = 0.8$ V and $I_{ds} = 20$ mA.

modeled T_{min} versus T_{ph} at constant $V_{DS} = 0.6$ V, $I_{DS} = 10$ mA and frequency of 6 GHz. In this plot, we also show the predicted trend of T_{min} if RST were absent and drain noise was therefore due solely to thermal noise from the channel resistance. This curve is obtained by setting $T_d = T_{el}$ in our noise model. We observe that under these bias conditions, the predicted T_{50} could vary linearly with T_{ph} rather than non-linearly, leading to relatively larger improvements in noise performance at room temperature compared to cryogenic temperature.

To examine this prediction in more detail, in Figs. 6b and 6c we plot the modeled T_{min} and the T_{min} predicted if the contribution of RST to T_d were suppressed at 40 K and 300 K, respectively. At 40 K, the modeled and predicted T_{min} exhibit a negligible difference for $V_{DS} \lesssim 0.6$ V, but at higher V_{DS} the predicted T_{min} is markedly less than the modeled value owing to the lack of noise from RST. The minimum of T_{min} at 40 K would improve by ~ 3 % if RST were suppressed. At 300 K, the difference between modeled and predicted T_{min} varies by up to ~ 40 % as V_{DS} is increased from 0.1 V to 1.0 V. In this case, the minimum T_{min} would improve by ~ 30 % in the absence of RST, suggesting that significant improvements in room temperature noise figure may be possible if RST is suppressed.

VI. CONCLUSION

We have characterized the S-parameters and the microwave noise temperature of InGaAs mHEMTs at 40 K and 300 K and various V_{DS}. At each T_{ph} and V_{DS}, we have extracted the drain temperature, T_d. From these data, we obtained the dependence of T_d on V_{DS} at 40 K and 300 K. T_d is found to exhibit a nonlinear trend with V_{DS} at both temperatures. We have introduced a model capable of explaining these trends in which drain noise originates from thermal noise of the channel resistance and RST of electrons from the channel to the barrier. The analysis indicates that at cryogenic temperatures and typical low-noise biases, thermal noise from the channel resistance is the main component of T_d in the present devices, while at 300 K, RST may account for over half of T_d. Further evidence for this model of drain noise may be obtained by observing how drain noise is affected by systematic variations in the channel and barrier compositions of HEMTs and hence conduction band offset.

ACKNOWLEDGMENT

The authors thank Sander Weinreb, Pekka Kangaslahti, Jacob Kooi, Jun Shi, Junjie Li, and Jan Grahn for useful discussions.

REFERENCES

[1] U. Mishra and J. Shealy, "InP-based HEMTs: status and potential," in *Proc. of Int. Conf. on Ind. Phos. and Rel. Mat.*, 1994, pp. 14–17.

[2] E. Bryerton, M. Morgan, and M. Pospieszalski, "Ultra low noise cryogenic amplifiers for radio astronomy," in *2013 IEEE Radio Wireless Symp.*, Jan. 2013, pp. 358–360.

[3] E. Cha, N. Wadefalk, G. Moschetti, A. Pourkabirian, J. Stenarson, and J. Grahn, "A 300-μW Cryogenic HEMT LNA for Quantum Computing," in *IEEE MTT-S Int. Microw. Symp*, Aug. 2020, pp. 358–360.

[4] E. Cha, N. Wadefalk, P.-. Nilsson, J. Schleeh, G. Moschetti, A. Pourkabirian, S. Tuzi, and J. Grahn, "0.314 and 1628 ghz Wide-Bandwidth Cryogenic MMIC Low-Noise Amplifiers," *IEEE Trans. Microw. Theory Tech.*, vol. 66, no. 11, pp. 4860–4869, 2018.

[5] W. R. Deal, K. Leong, V. Radisic, S. Sarkozy, B. Gorospe, J. Lee, P. H. Liu, W. Yoshida, J. Zhou, M. Lange, R. Lai, and X. B. Mei, "Low noise amplification at 0.67 thz using 30 nm inp hemts," *IEEE Microw. Wirel. Compon. Lett.*, vol. 21, no. 7, pp. 368–370, 2011.

[6] F. Thome, F. Schfer, S. Trk, P. Yagoubov, and A. Leuther, "A 67-116-GHz Cryogenic Low-Noise Amplifier in a 50-nm InGaAs Metamorphic HEMT Technology," *IEEE Microw. Wirel. Compon. Lett*, pp. 1–4, 2021.

[7] D. Cuadrado-Calle, D. George, G. A. Fuller, K. Cleary, L. Samoska, P. Kangaslahti, J. W. Kooi, M. Soria, M. Varonen, R. Lai, and X. Mei, "Broadband MMIC LNAs for ALMA Band 2+3 With Noise Temperature Below 28 K," *IEEE Trans. Microw. Theory Tech.*, vol. 65, no. 5, pp. 1589–1597, May 2017.

[8] M. Pospieszalski, "Modeling of noise parameters of mesfets and modfets and their frequency and temperature dependence," *IEEE Trans. Microw. Theory Tech.*, vol. 37, no. 9, pp. 1340–1350, 1989.

[9] M. W. Pospieszalski, "On the limits of noise performance of field effect transistors," in *IEEE MTT-S Int. Microw. Symp*, 2017, pp. 1953–1956.

[10] F. Heinz, F. Thome, D. Schwantuschke, A. Leuther, and O. Ambacher, "A Scalable Small-Signal and Noise Model for High-Electron-Mobility Transistors Working Down to Cryogenic Temperatures," *IEEE Trans. Microw. Theory Tech.*, vol. 70, no. 2, pp. 1097–1110, Feb. 2022.

[11] B. Gabritchidze, K. Cleary, J. Kooi, I. Esho, A. C. Readhead, and A. J. Minnich, "Experimental characterization of temperature-dependent microwave noise of discrete hemts: Drain noise and real-space transfer," in *IEEE MTT-S Int. Microw. Symp. Dig.*, 2022, pp. 615–618.

[12] I. Esho, A. Y. Choi, and A. J. Minnich, "Theory of drain noise in high electron mobility transistors based on real-space transfer," *J. Appl. Phys.*, vol. 131, no. 8, p. 085111, Feb. 2022.

[13] J. Shah, "Hot carriers in quasi-2-d polar semiconductors," *IEEE Journal of Quantum Electronics*, vol. 22, no. 9, pp. 1728–1743, 1986.

[14] H. Hartnagel, R. Katilius, and A. Matulionis, *Microwave Noise in Semiconductor Devices*, 1st ed. NY, USA: Wiley-Intersci. Ser., 2001.

[15] M. Murti, J. Laskar, S. Nuttinck, S. Yoo, A. Raghavan, J. Bergman, J. Bautista, R. Lai, R. Grundbacher, M. Barsky, P. Chin, and P. Liu, "Temperature-dependent small-signal and noise parameter measurements and modeling on InP HEMTs," *IEEE Trans. Microw. Theory Tech.*, vol. 48, no. 12, pp. 2579–2587, 2000.

[16] S. Weinreb and J. Shi, "Low Noise Amplifier With 7-K Noise at 1.4 GHz and 25 C," *IEEE Trans. Microw. Theory Tech.*, vol. 69, no. 4, pp. 2345–2351, 2021.

[17] M. W. Pospieszalski and A. C. Niedzwiecki, "FET noise model and on-wafer measurement of noise parameters," in *IEEE MTT-S Int. Microw. Symp. Dig.*, July 1991, pp. 1117–1120 vol.3.

[18] J. Schleeh, H. Rodilla, N. Wadefalk, P.-. Nilsson, and J. Grahn, "Characterization and Modeling of Cryogenic Ultralow-Noise InP HEMTs," *IEEE Trans. Electron Devices*, vol. 60, pp. 206–212, Jan. 2013.

[19] F. Heinz, F. Thome, A. Leuther, and O. Ambacher, "Noise Performance of Sub-100-nm Metamorphic HEMT Technologies," in *IEEE MTT-S Int. Microw. Symp*, Aug. 2020, pp. 293–296.

[20] D. Russell, K. Cleary, and R. Reeves, "Cryogenic probe station for on-wafer characterization of electrical devices," *Rev. Sci. Instrum.*, vol. 83, no. 4, p. 044703, 2012.

[21] J. Fernandez, "A Noise Temperature Measurement System Using a Cryogenic Attenuator," *TMO Prog. Rep.*, no. 42, p. 135, 1998.

[22] G. Dambrine, A. Cappy, F. Heliodore, and E. Playez, "A new method for determining the fet small-signal equivalent circuit," *IEEE Trans. Microw. Theory Tech.*, vol. 36, no. 7, pp. 1151–1159, 1988.

[23] M. Berroth and R. Bosch, "Broad-band determination of the fet small-signal equivalent circuit," *IEEE Trans. Microw. Theory Tech.*, vol. 38, no. 7, pp. 891–895, 1990.

[24] P. Hower and N. Bechtel, "Current saturation and small-signal characteristics of GaAs field-effect transistors," vol. 20, no. 3, pp. 213–220.

[25] A. R. Alt and C. R. Bolognesi, "(inp) hemt small-signal equivalent-circuit extraction as a function of temperature," *IEEE Trans. Microw. Theory Tech.*, vol. 63, no. 9, pp. 2751–2755, 2015.

[26] A. H. Akgiray, "New Technologies Driving Decade-Bandwidth Radio Astronomy: Quad-ridged Flared Horn and Compound-Semiconductor LNAs," Ph.D. dissertation, Cal. Inst. of Tech., Pasadena, CA, USA, 2013.

[27] G. Kompa, *Parameter Extraction and Complex Nonlinear Models*. Norwood MA: Artech House, 2020.

[28] M. W. Pospieszalski, "Extremely low-noise amplification with cryogenic FETs and HFETs: 1970-2004," vol. 6, no. 3, pp. 62–75.

[29] J. Schleeh, J. Mateos, I. iguez-de-la Torre, N. Wadefalk, P. A. Nilsson, J. Grahn, and A. J. Minnich, "Phonon black-body radiation limit for heat dissipation in electronics," *Nat. Mater*, vol. 14, no. 2, pp. 187–192.

[30] D. C. Ruiz, T. Saranovac, D. Han, O. Ostinelli, and C. Bolognesi, "Impact ionization control in 50 nm low-noise high-speed inp hemts with inas channel insets," in *2019 IEEE International Electron Devices Meeting (IEDM)*, 2019, pp. 9.3.1–9.3.4.

[31] C.-Y. Chang, H.-T. Hsu, E. Y. Chang, C.-I. Kuo, S. Datta, M. Radosavljevic, Y. Miyamoto, and G.-W. Huang, "Investigation of impact ionization in inas-channel hemt for high-speed and low-power applications," *IEEE Electron Device Lett.*, vol. 28, no. 10, pp. 856–858, 2007.

[32] J. Huang, T. Y. Chang, and B. Lalevic, "Measurement of the conductionband discontinuity in pseudomorphic InxGa1xAs/in0.52al0.48as heterostructures," *Appl. Phys. Lett.*, vol. 60, no. 6, pp. 733–735.

[33] P. E. Longhi, L. Pace, S. Colangeli, W. Ciccognani, and E. Limiti, "Technologies, design, and applications of low-noise amplifiers at millimetre-wave: State-of-the-art and perspectives," vol. 8, no. 11, p. 1222, number: 11.

[34] J. Schleeh, "Ultra-Low Noise InP HEMTs for Cryogenic Amplification," Ph.D. dissertation, Chalm. Univ. of Tech., Got. Sweden, 2012.